Radio interferometry in astronomy: a view into the XXI century

Lecture 2

Radio galaxies, AGN, quasars

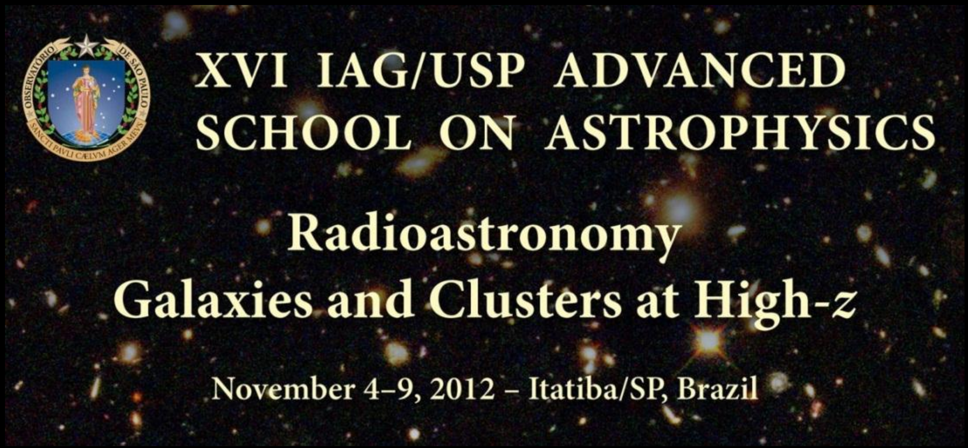

Leonid Gurvits

JOINT INSTITUTE FOR VLBI IN EUROPE

TU Delft

Joint Institute for VLBI in Europe, Dwingeloo, The Netherlands

Delft University of Technology, Faculty of Aerospace Engineering, The Netherlands

His majesty synchrotron

Extragalactic sky in pre-radio astronomy era

Optical astronomy in the 1930s

- Milky Way
- Nearby Galaxies

(out to a few Mpc)

Hubble Law: $D=c*z/Ho$

The synchrotron extragalactic sky

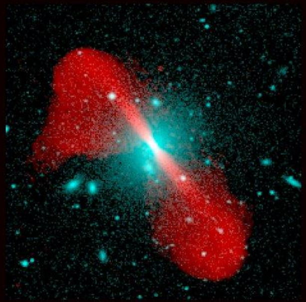

Radio Galaxy 3C296
Radio/optical superposition

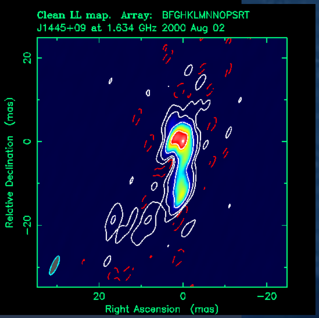

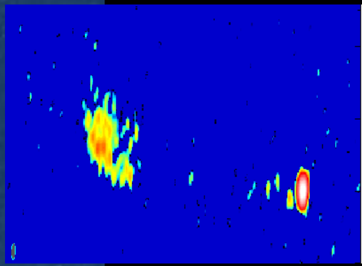

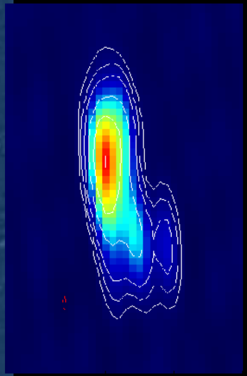

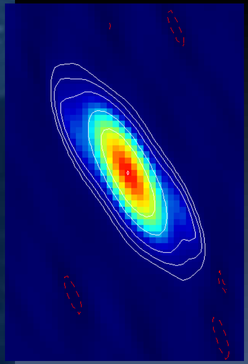

Optical versus radio views at the same objects

Centaurus A:
5 Mpc from Milky Way

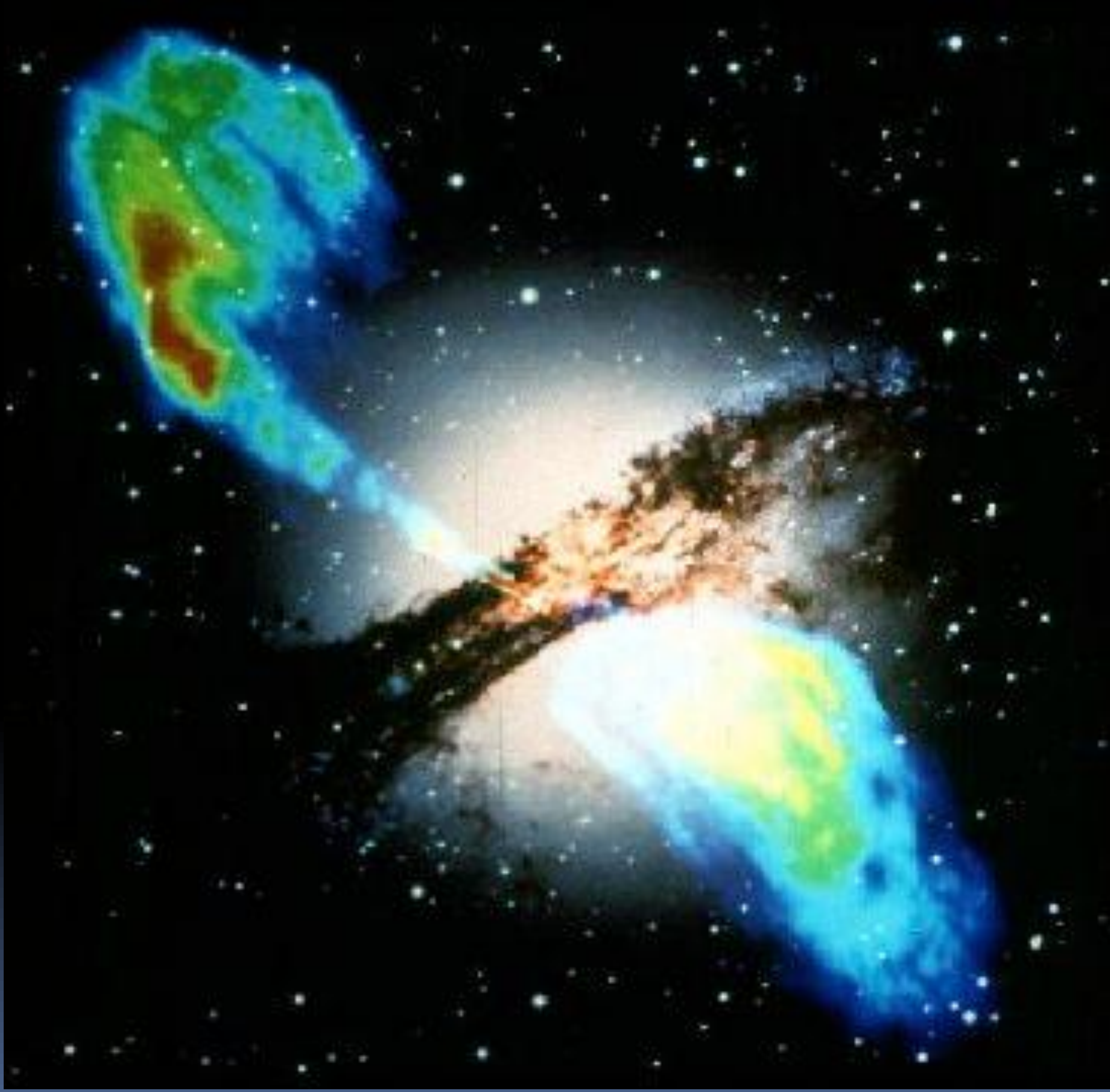

Power-law emission spectra

- Polarisation
- High Brightness Temp
- Synchrotron radiation of relativistic electrons in magnetic fields

AGN: expectations versus observational facts

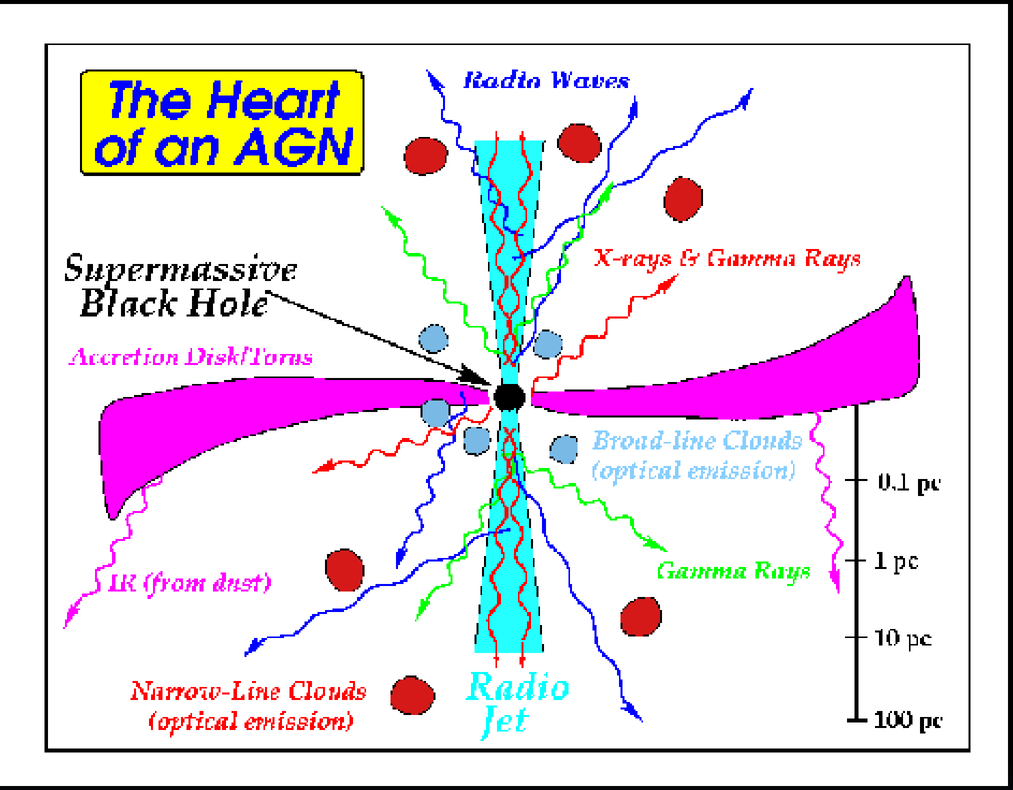

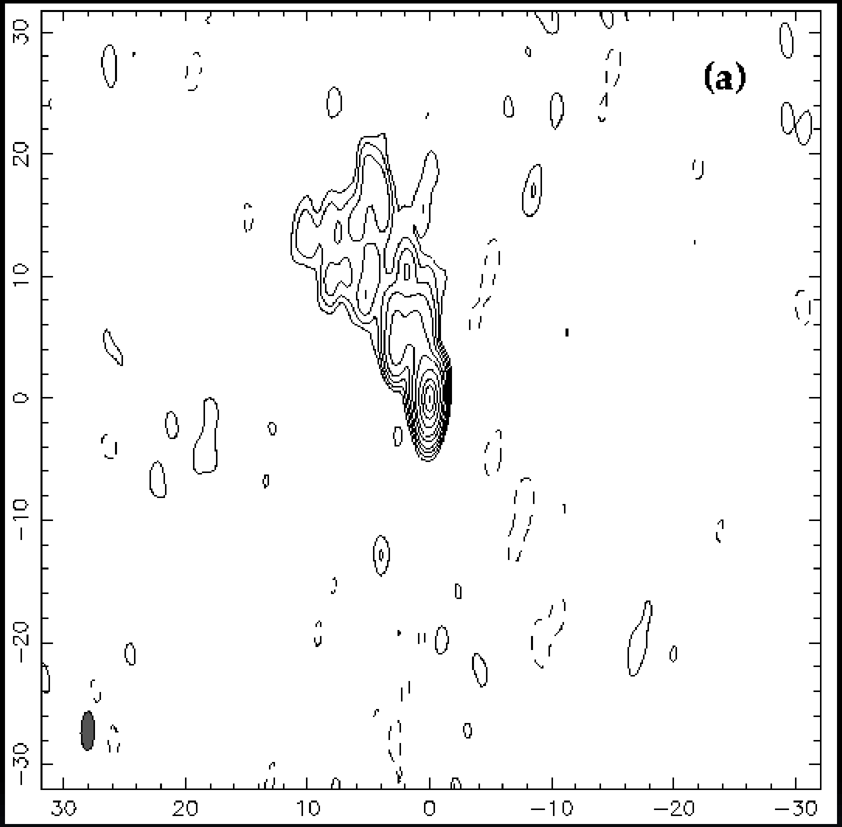

ARISE, 1999, JPL Publ. 99-14

- **What is the correspondence between the two pictures (jets, cores, etc.)?**
- **How much deeper in the "core" can one go (a hunt for the highest T_B)?**

What are jets made of?

AGN as seen in radio: what's so special?

- Advantage of radio domain (among others): high angular resolution

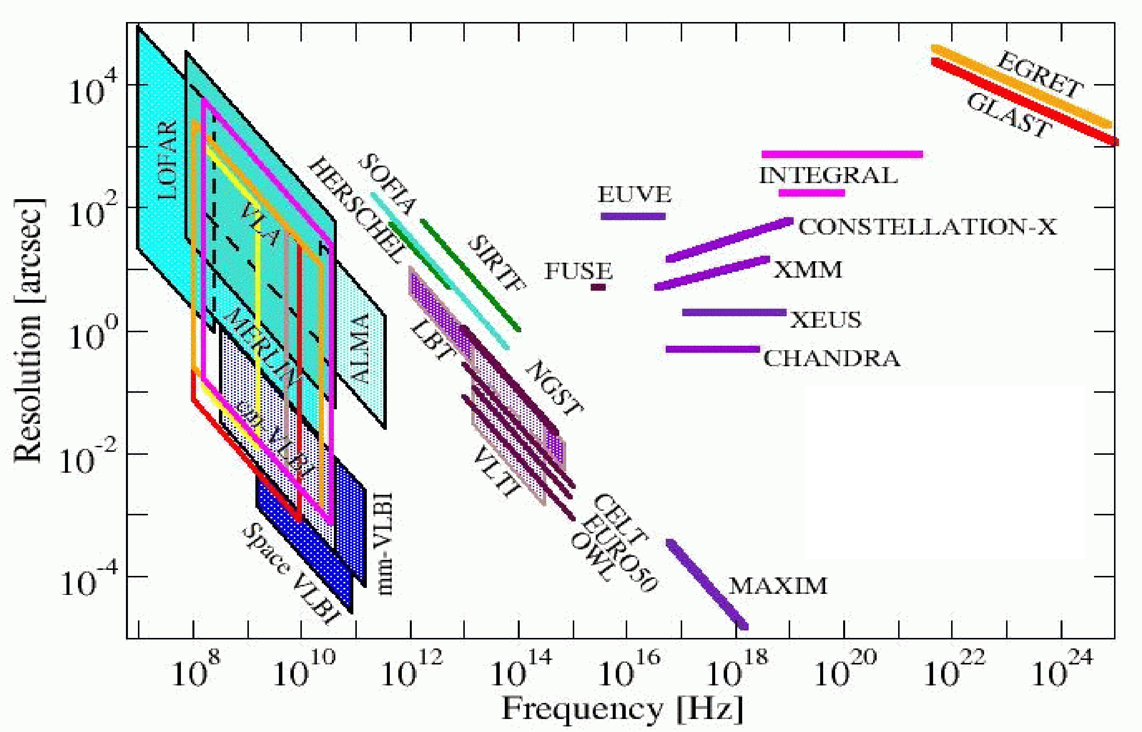

λ ← 3 cm 3 μm 3 Å

- Disadvantage: dealing with a "smoking gun"

1156+295: a show case of helical jet (HPQ at z=0.729)

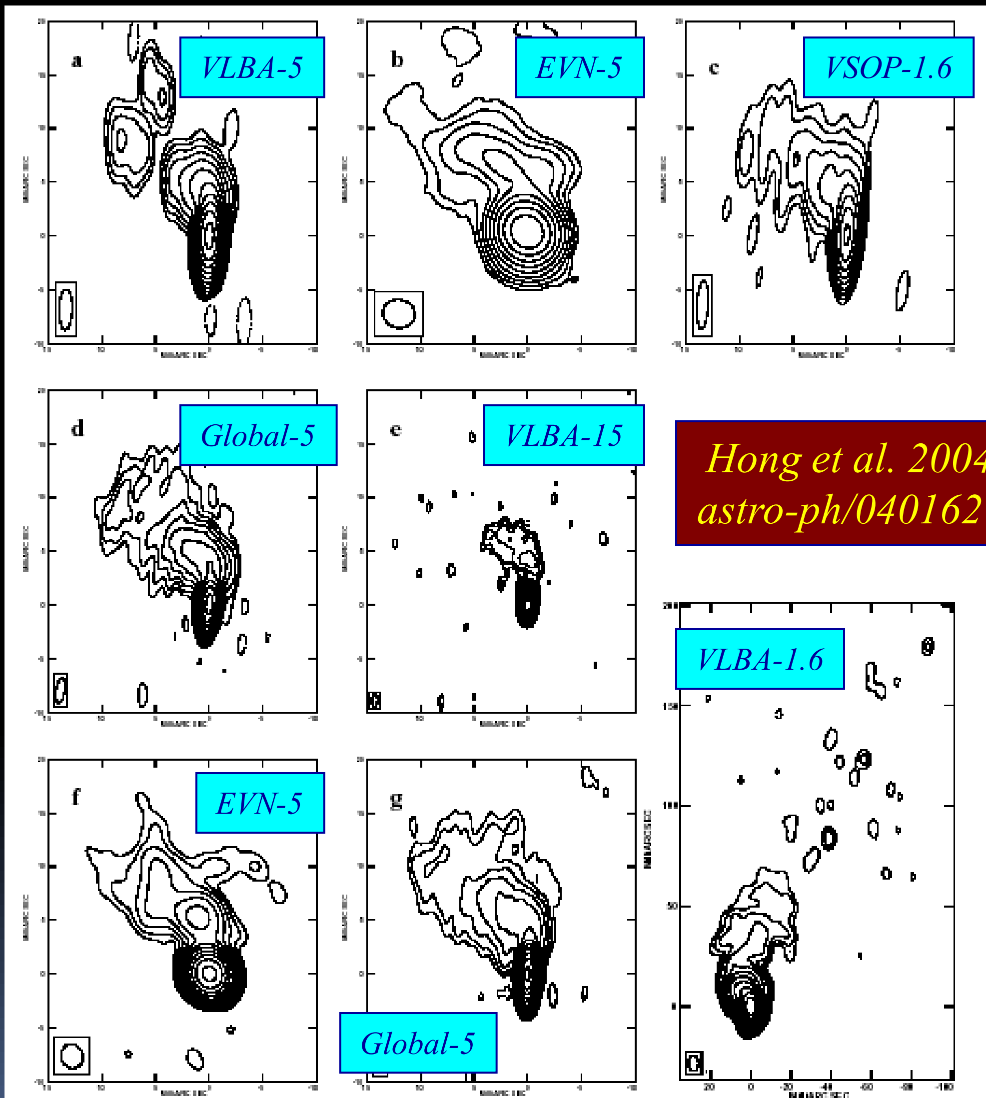

Hong et al. 2004
astro-ph/0401627

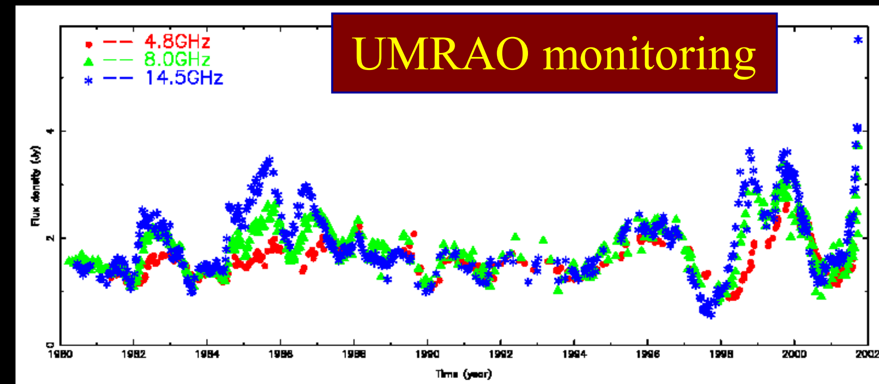

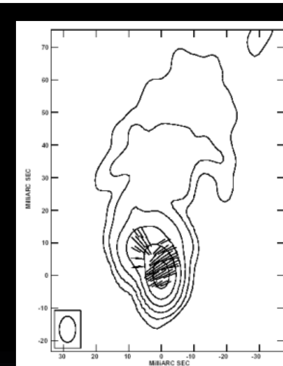

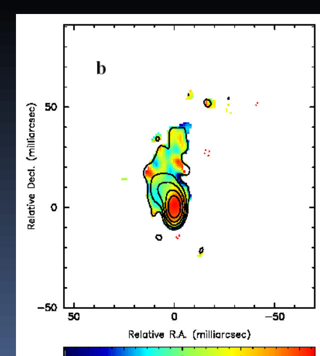

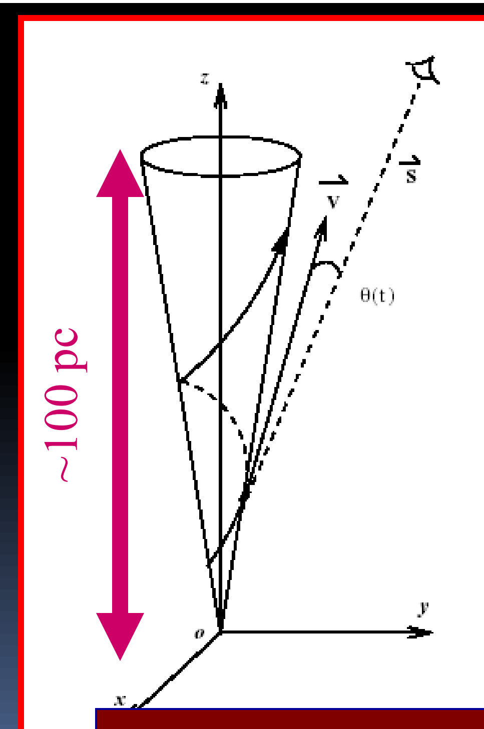

Best-fit model

Jets in AGN – relativistic objects

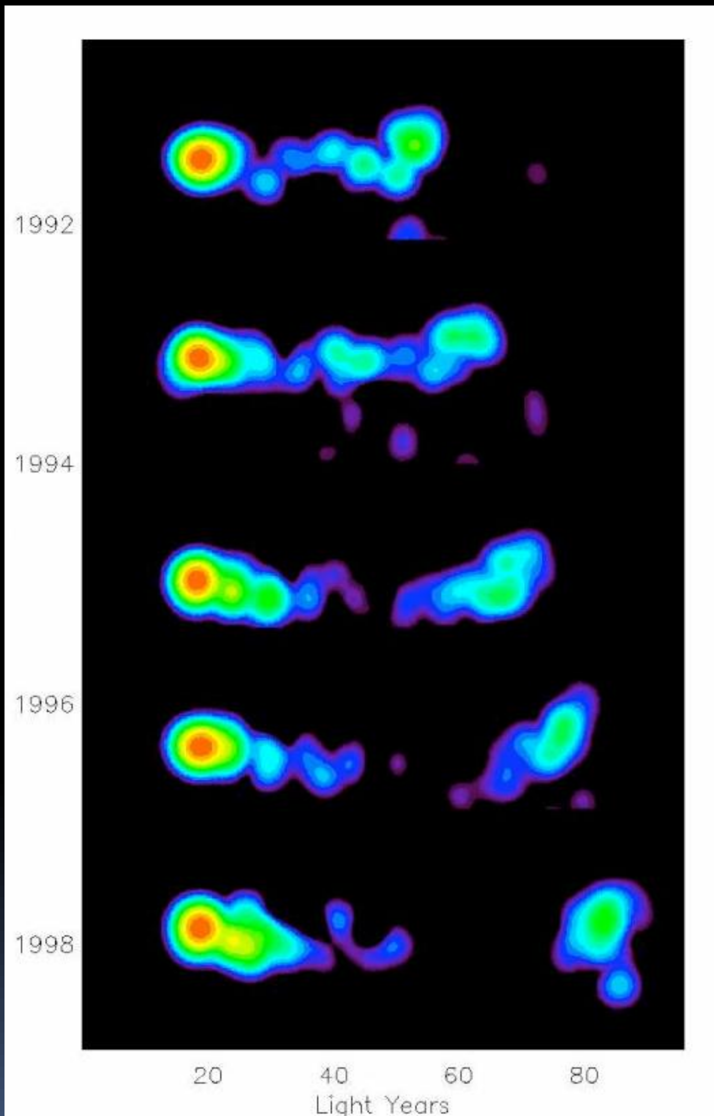

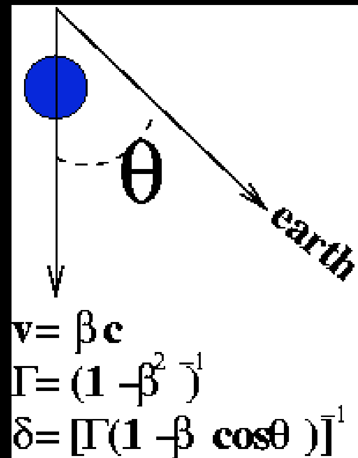

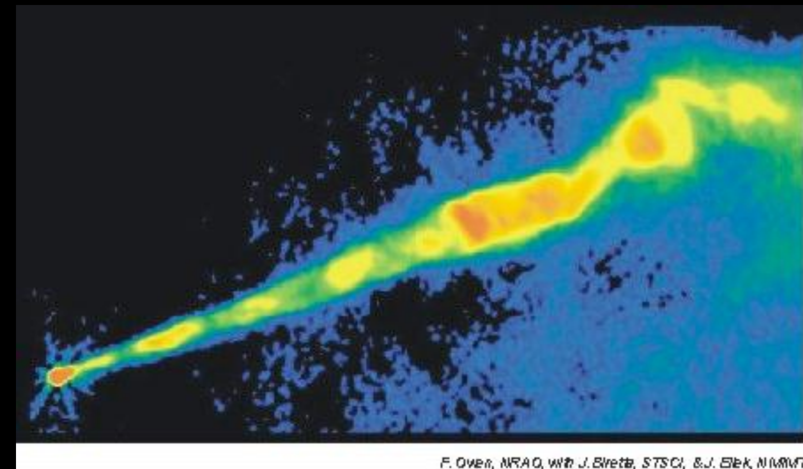

$$v_{app} = v\ sin\theta/(1\text{-}\beta cos\theta)$$

For certain combinations of v and θ, v_{app} can be greater than c !

NGC4258: the most convincing case for a super-massive black hole

(Miyoshi et al. 1995, Nat 373, 127; Herrnstein et al. 1998, ApJ 497, L69)

Rotating gas near the centre of the galaxy NGC4258, as traced by VLBI observations of the water vapor maser line at 22 GHz (1.35 cm)

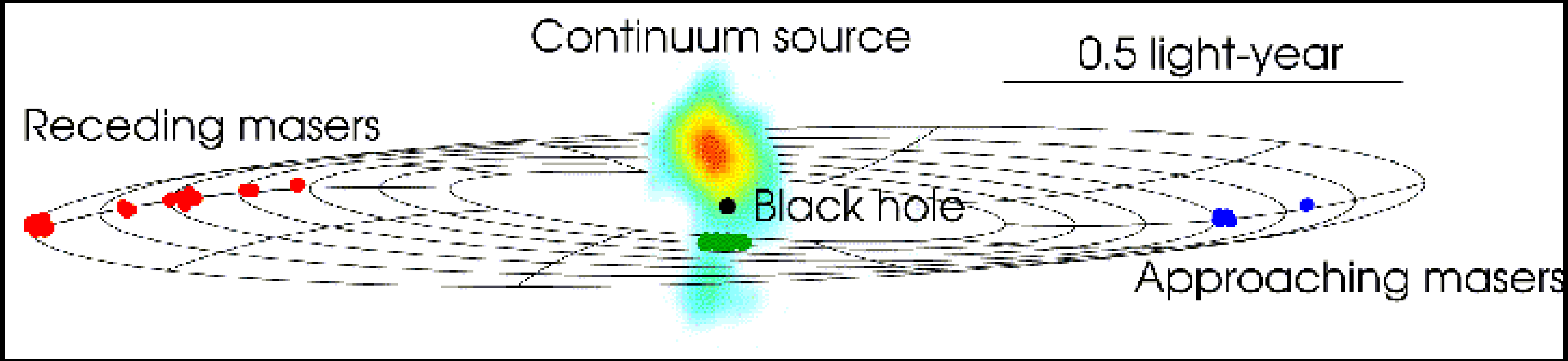

Doppler measurements → **Radial velocities**

VLBI measurements → **(Angular) radii**

$$V^2 / R \longrightarrow 3.6\times10^7 M_{\rm sun} \text{ within } R = 0.13\,\text{pc}$$

2215+020 (z=3.55): jet resolved by VSOP

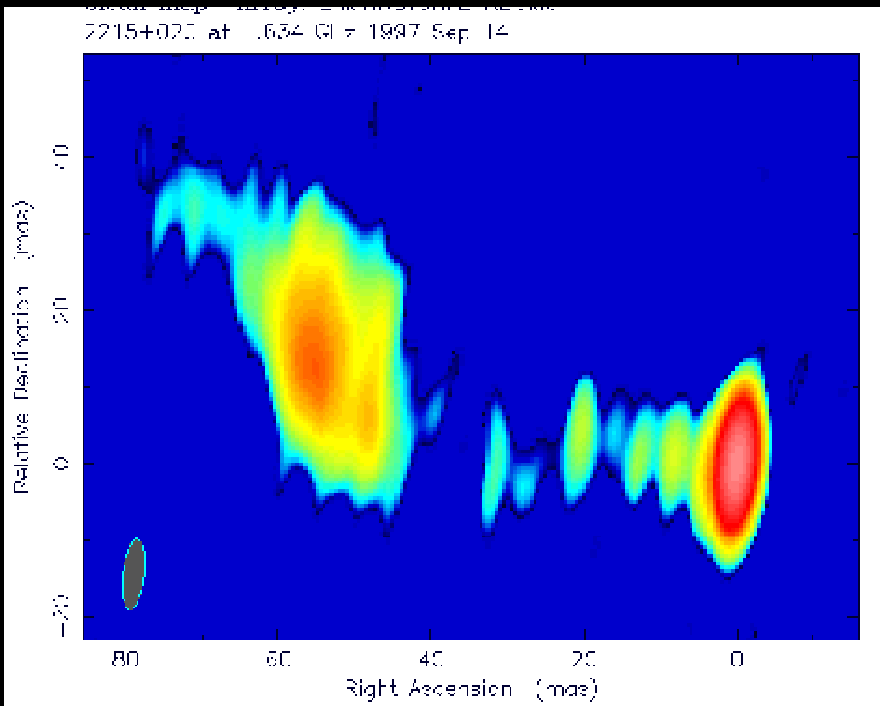

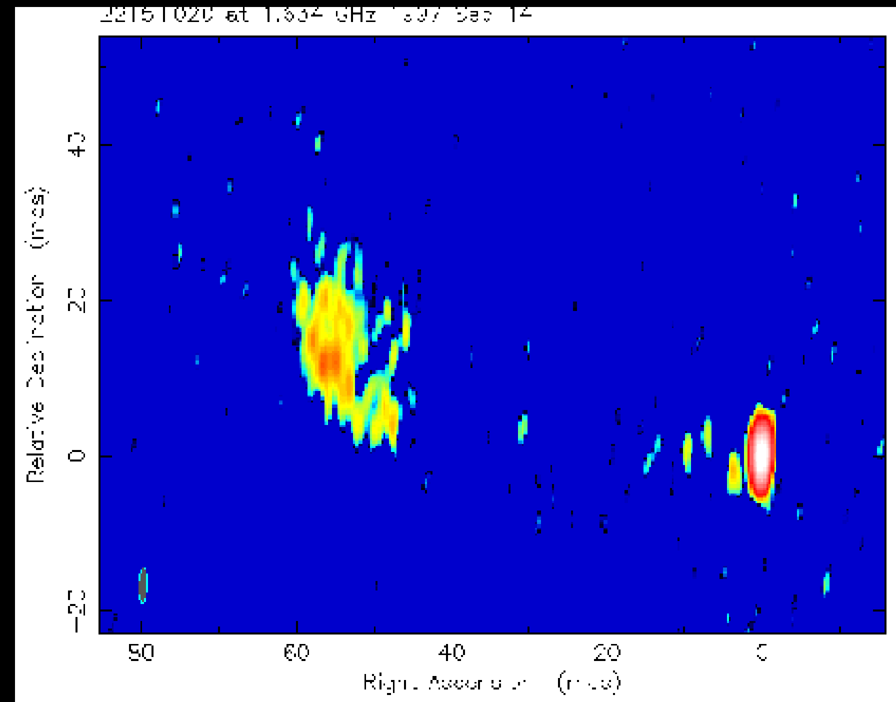

- Cross-section of the jet appears resolved: $5 \leq \theta_{jet} \leq 9 \text{ mas}$
- Theoretical prediction for jet cross-section (Beskin 1997):

$$r_{\mathrm{jet}} \approx 3\times 10^{5}\,\frac{M_{\mathrm{BH}}}{M_{\mathrm{o}}}\left(\frac{B_{\mathrm{in}}}{B_{\mathrm{ext}}}\right)^{0.5}\,[\mathrm{cm}]$$

2215+020 (z=3.55): jet cross-section resolved

$B_{\rm ext} = 10^{-5}$ G (Beck 2000)

$B_{\rm in} = 10^{4}$ G (Field & Rogers)

$r_{\rm jet} \approx 20 h^{-1}$ pc

$M_{\rm BH} \cong 6 \times 10^9 h^{-1} M_{\rm o}$

Potentially powerful method for estimating $M_{\rm BH}$ in AGN, especially in statistical studies

Lobanov et al. 2001

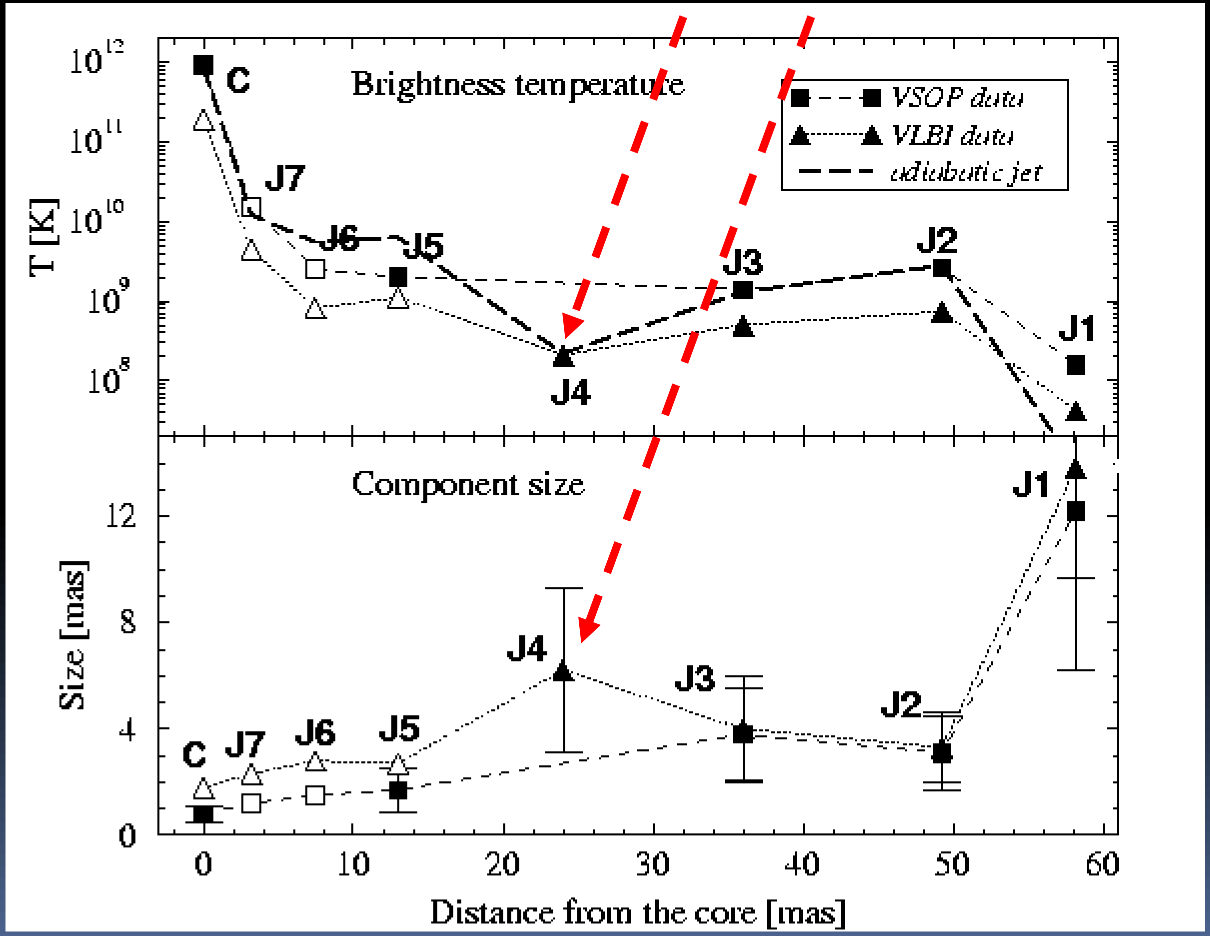

Resolving jet cross-section: VSOP at its best

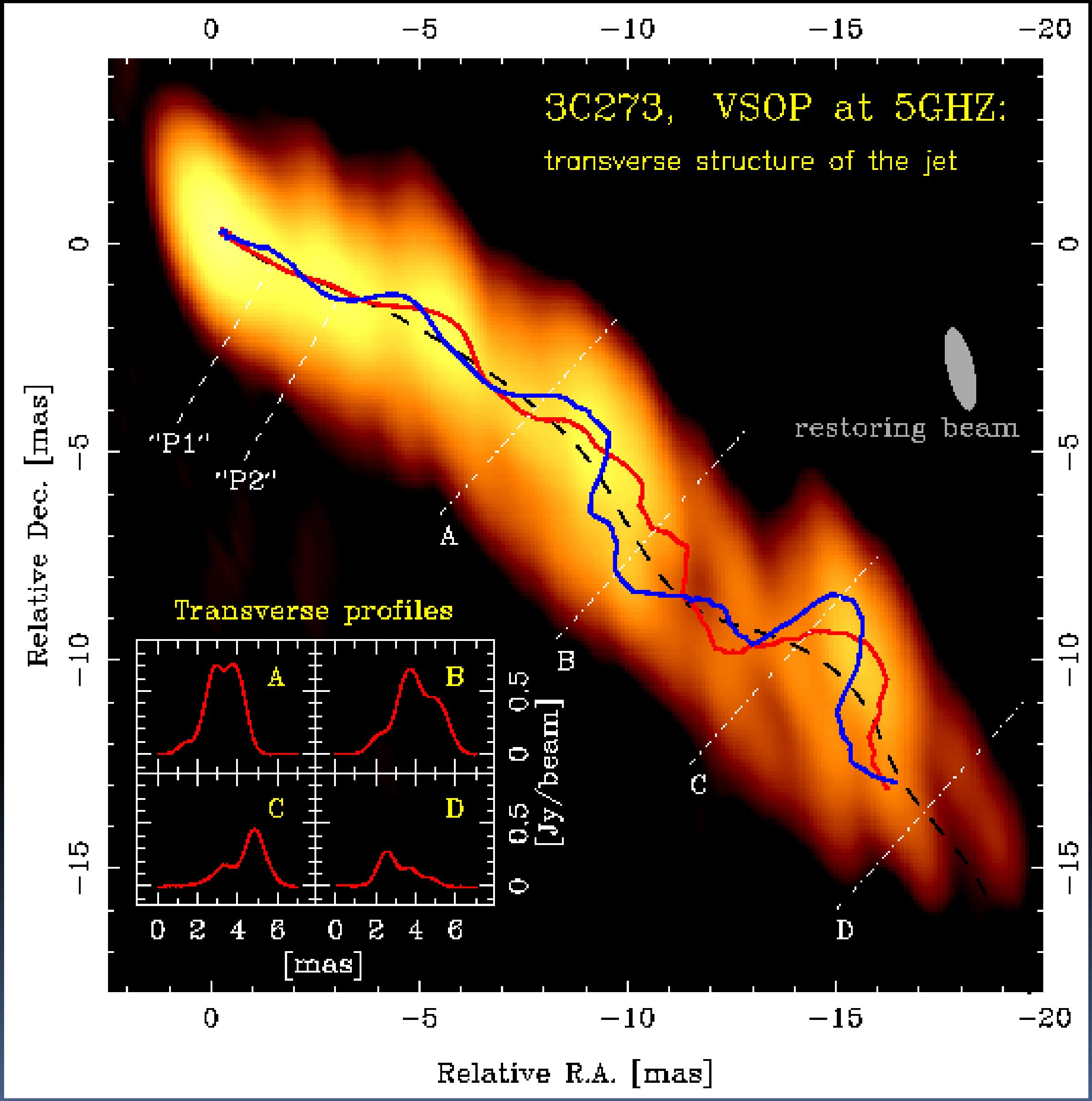

3C273, 6 cm, VSOP

Lobanov & Zensus 2000

Imagine non-imaged…

Imaging versus non-imaging analysis

Van Cittert – Zernike theorem (optics analogy):

$$V(u,v) = \int_{-\infty}^{+\infty}\int_{-\infty}^{+\infty} I(x,y)e^{i2\pi(ux+vy)}dxdy$$

Visibility function

Brightness distribution

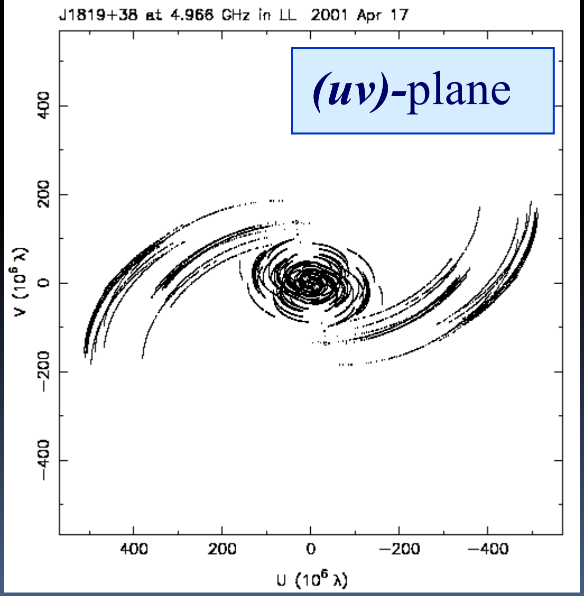

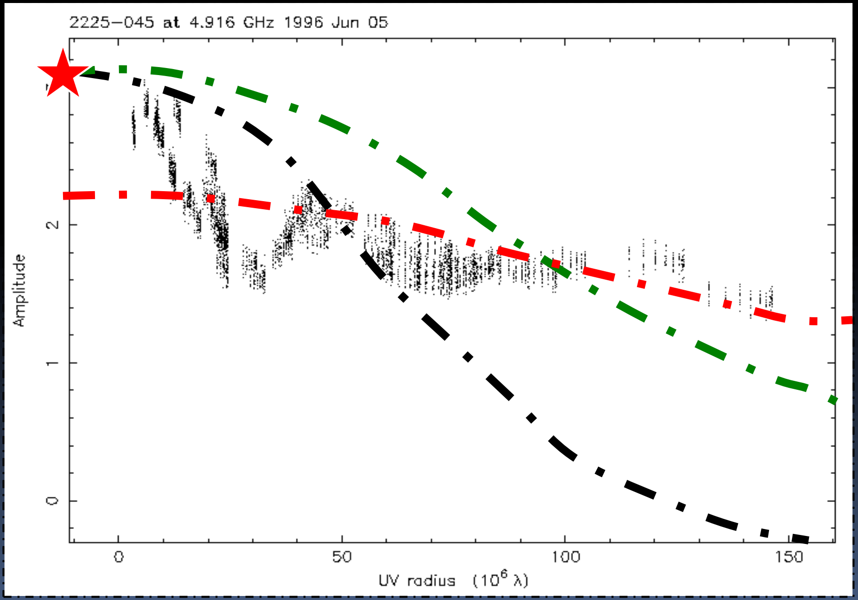

Visibility amplitude

Projected baseline

How much remains unresolved?

Combined data: VLBApls and VSOP Survey, 98 sources

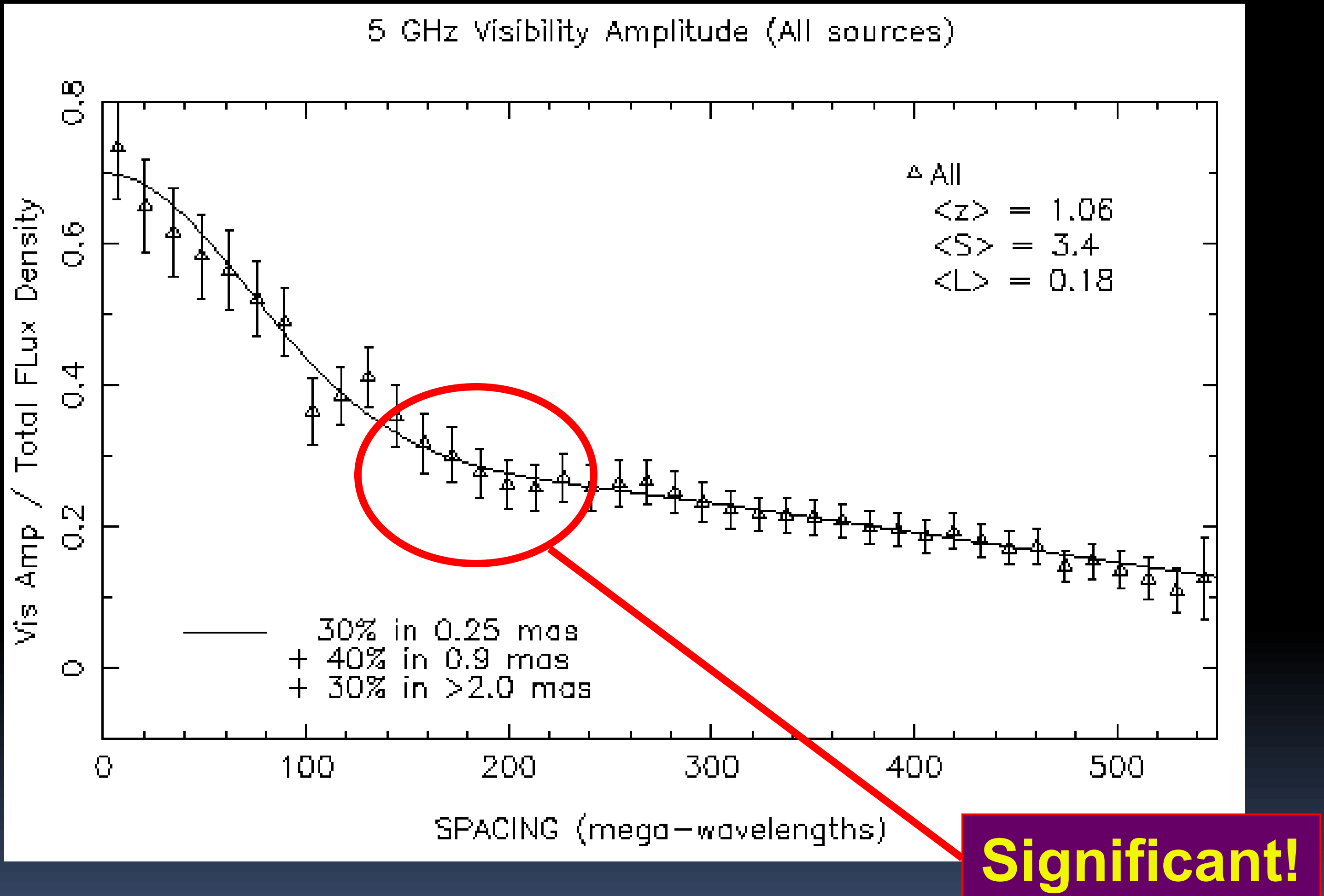

VSOP Survey publications, Horiuchi et al. 2004

The challenge: to mine the terra incognita

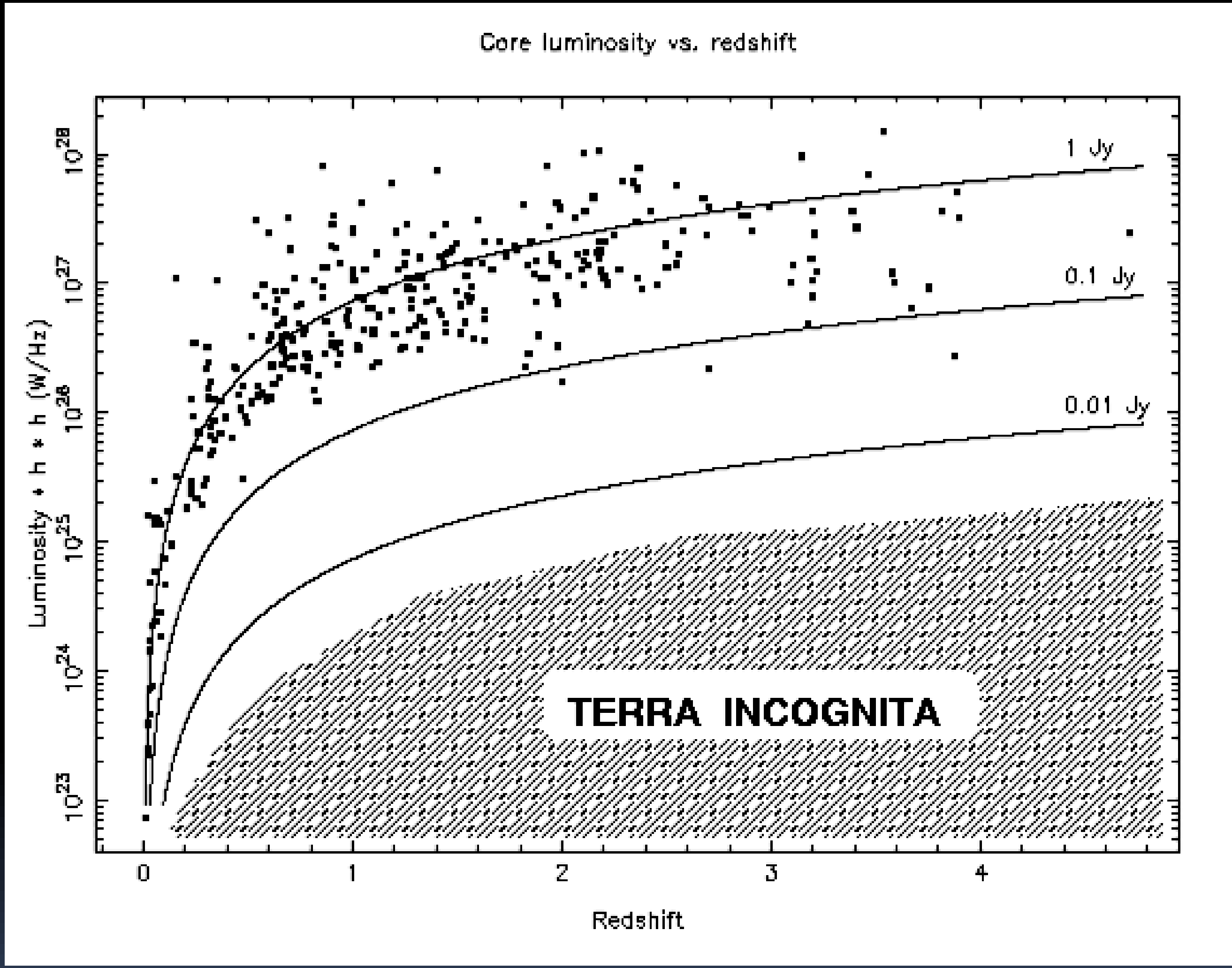

Need to observe mJy-level sources to study 10^{23} – 10^{25} W/Hz objects at z>0.5

Why bother? – Many reasons: e.g. cosmological applications

VLBI Surveys of AGN

VSOP/VLBA Pre–launch Survey of Extragalactic Radio Sources at 5 GHz (VLBApls)

E.B.Fomalont [1], S.Frey [2], Z.Paragi [2], L.I.Gurvits [3], W.K.Scott [4], A.R.Taylor [4], P.G.Edwards [5], H.Hirabayashi [5]

[1] National Radio Astronomy Observatory, Charlottesville, VA, USA
[2] FOMI Satellite Geodetic Observatory, Penc, Hungary
[3] Joint Institute for VLBI in Europe, Dwingeloo, The Netherlands
[4] University of Calgary, Alberta, Canada
[5] Institute of Space and Astronautical Science, Sagamihara, Japan

Observed 05–06 June 1996. Axes marked in milliarcseconds.

Astrophysical Journal Supplement, 2000

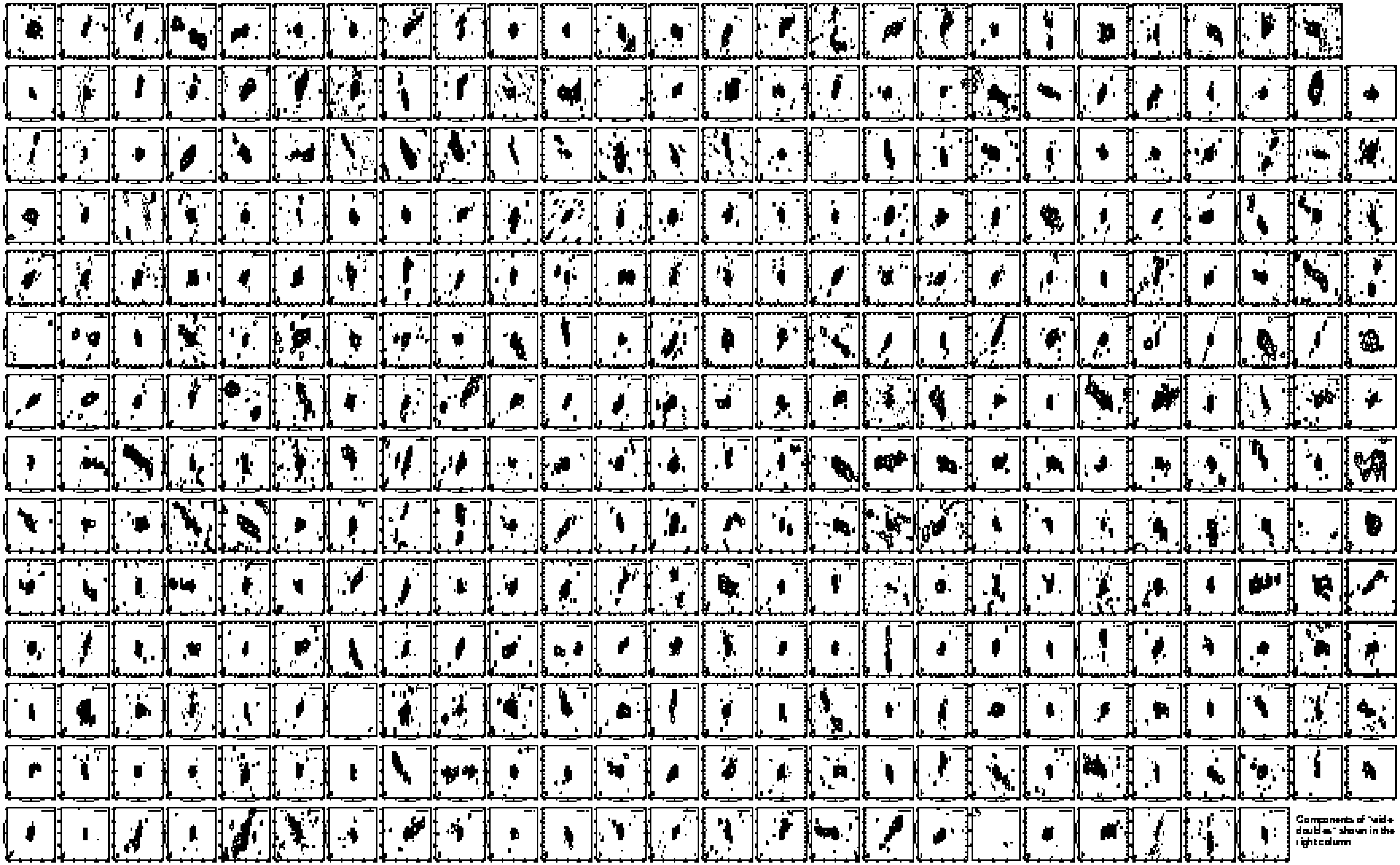

Components of "wide doubles" shown in the right column

Angular size – redshift (θ–z) tests: the concept

- First proposal:
  F.Hoyle, 1959, URSI S.#1 / IAU S.#9, Paris

- Many attempts to use arc-second scale radio structures as standard rods

But:

  - *first attempts (Kapahi 1987, Barthel and Miley 1988,, Nilsson et al 1993, and others) encountered strong source evolution*

  - *some encouraging results recently by Buchalter et al. 1998, Daly et al. 2001, 2002*

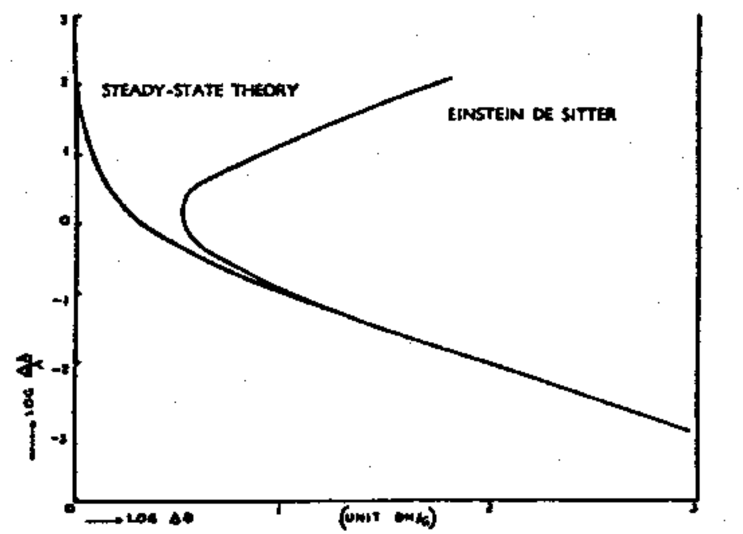

FIG. 5. Apparent diameter Δθ of a source of absolute diameter *D*, plotted against red-shift.

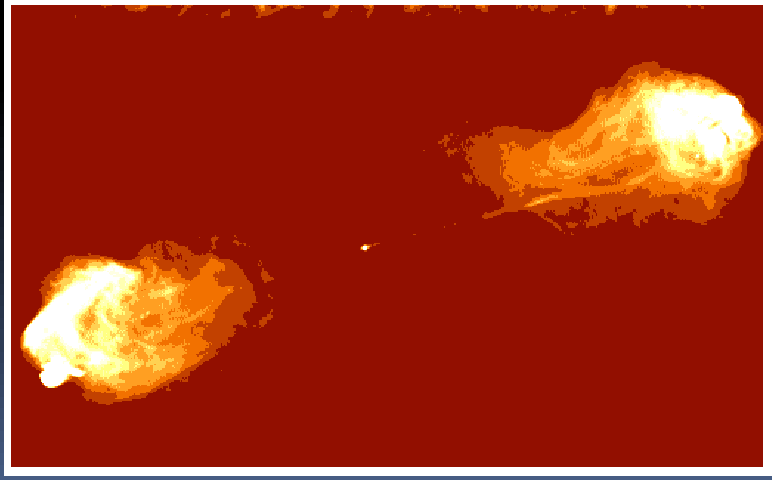

Angular size – redshift (θ–z) tests: early days

- "Sub-arcsecond Radio Astronomy" conference, Manchester, 1992: Demonstration attempts to use parsec-scale cores as standard rods (Kellermann 1992, 93; LIG 1992, 94)

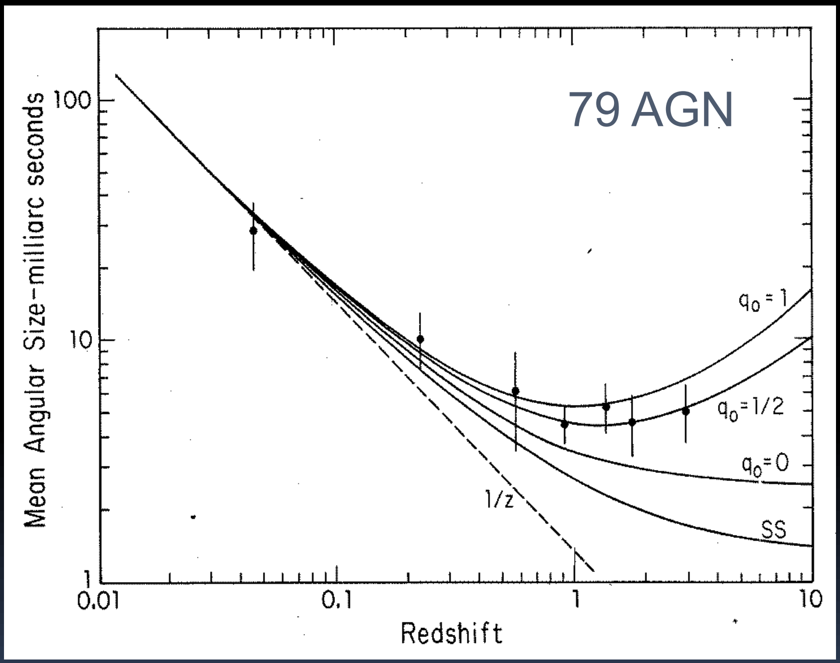

Kellermann 1993

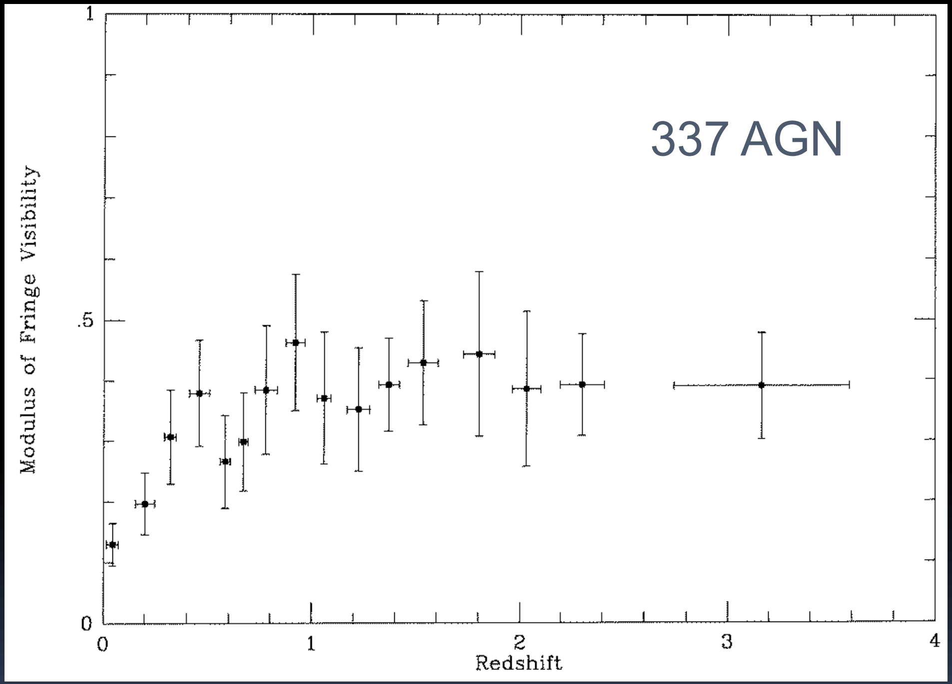

LIG 1993,
data by Preston et al. 1985

θ-z in 2000: "maximum" use of ad-hoc data

- 330 sources with known redshift and mas images at 5 GHz better than 100:1

- 4-parameter regression model ("proof of suitability")

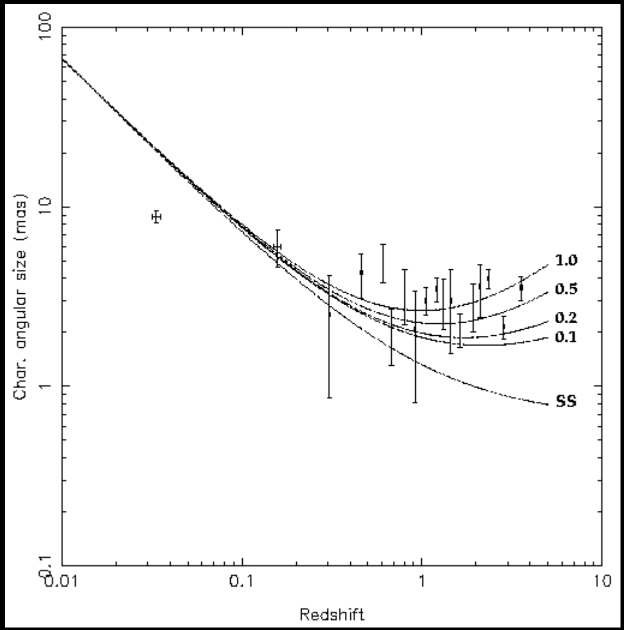

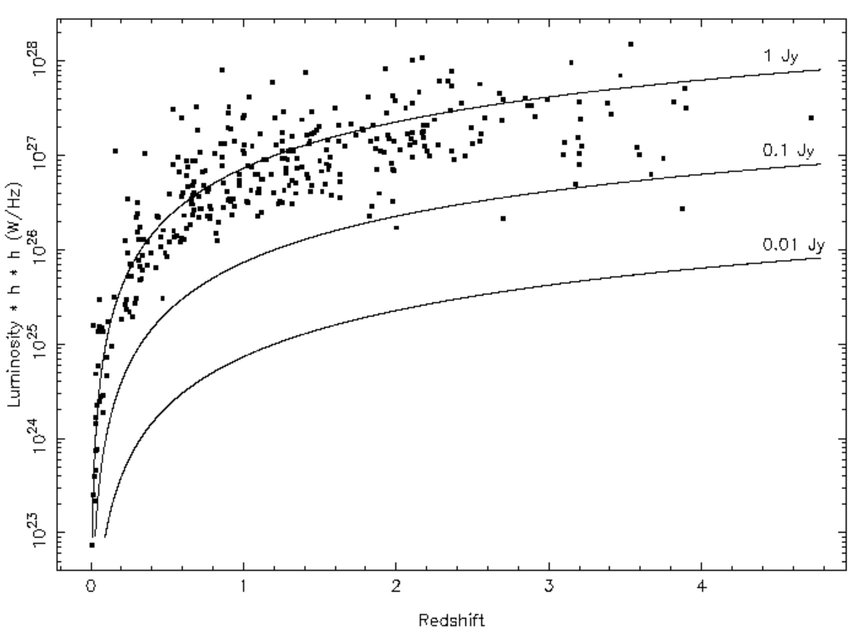

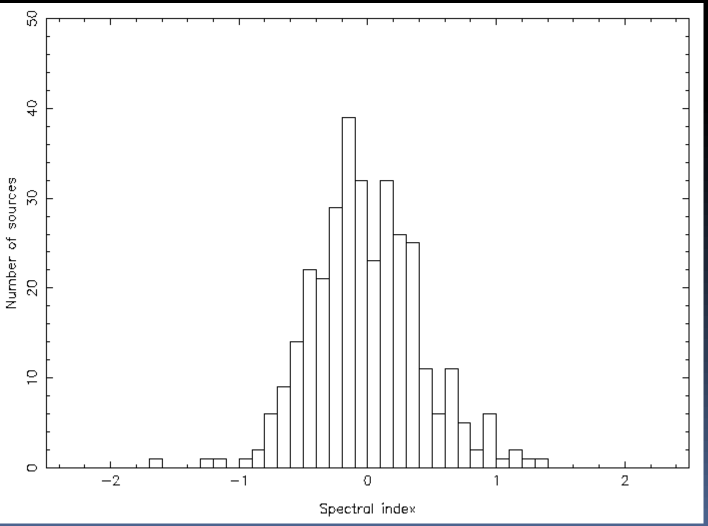

LIG, Kellermann, Frey 1999

Aftermath of the "maximum use" sample publication

Vishwakarma 2001 a,b
Astro-ph/9912105, -/0012492,

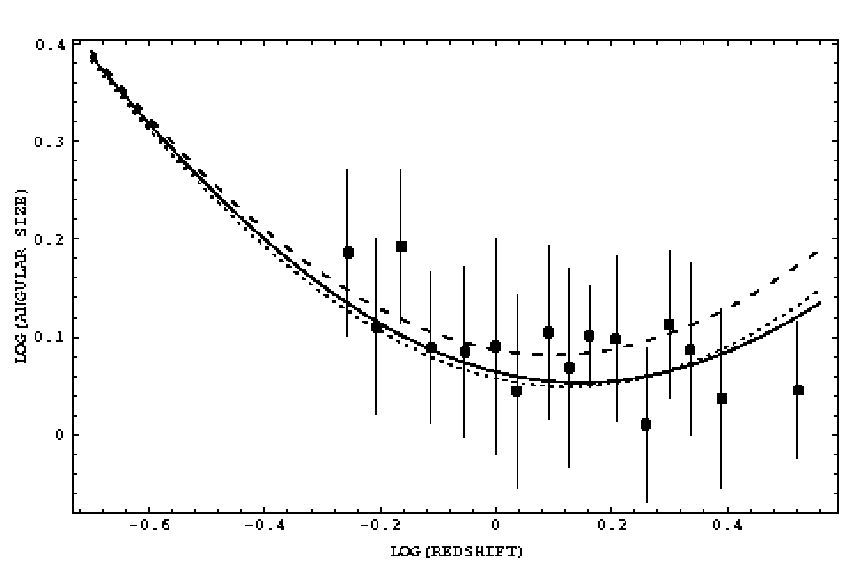

- Re-analysed data from LIG 1994 (256 sources) and LIG, Kellermann and Frey 1999 (330 sources) in concurrence with the Type Ia SN (Riess 1998, Perlmutter et al. 1999)
- Various models analyzed:

$$1+\Omega_{ko}=\Omega_0+\Omega_{\Lambda 0},\quad 2[q_0+\Omega_{\Lambda 0}]=\Omega_0$$

models	Ω_0 flat	Ω_0 global	$\Omega_{\Lambda 0}$ global
$\Lambda\sim S^{-2}$	0.68	0.97	0.61
$\Lambda\sim H^2$	0.67	0.29	1.03
$\Lambda\sim\rho$	0.67	0.53	0.82
Λ=const	0.2	0.08	1.16

θ-z data favor accelerating and decelerating models with $\Lambda=var$ or accelerating models with $\Lambda=const$ (SN Ia data: acceleration in both cases)

Aftermath of the "maximum use" sample publication

Lima & Alcaniz 2002

- FRW model driven by non-relativistic matter and a smooth "dark energy" component $p_x = \omega \rho_x$
- Best fit

$$\Omega_m \leq 0.62, \quad \omega \leq -0.2, \quad lh = 20 \ \text{pc}$$
$$\Omega_m \leq 0.17, \quad \omega \leq -0.65, \quad lh = 20 \ \text{pc}$$

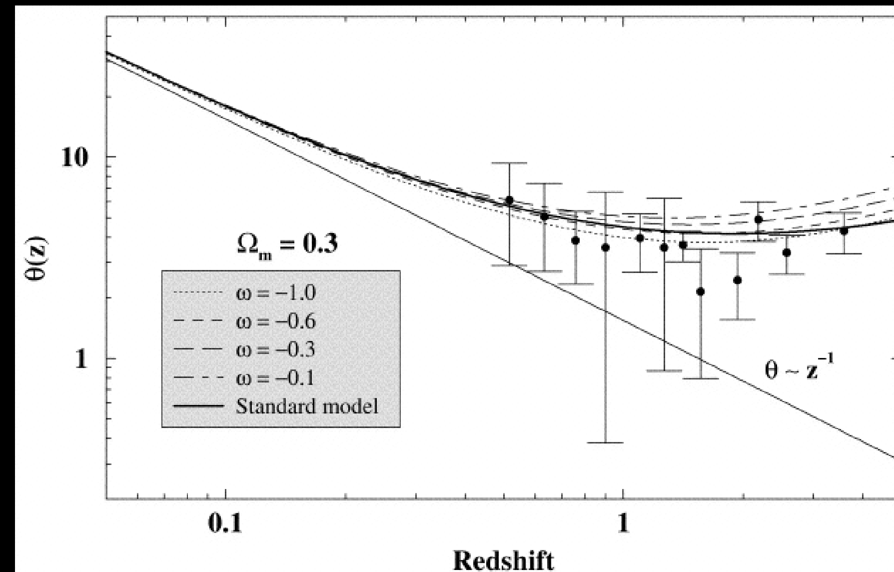

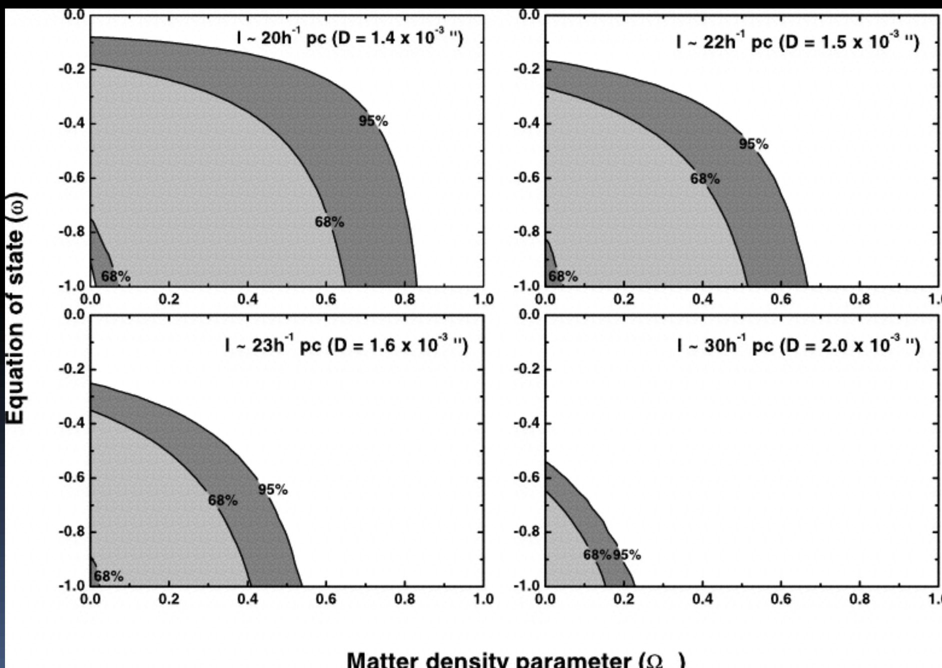

Conventional flat ΛCDM model ($\omega = -1$) with $\Omega_m = 0.2$ is the best fit.

Better statistics –

– more ata needed!

$\theta - z$ studies today: conclusions so far

- Provide consistency check with other cosmological tests (CMB, SN Ia in particular)
- Confirm preference of Λ-term or "dark energy" dominated models
- Will do much better with better statistics (more sources)
- Will serve as an additional input in the "Cosmic complementarity" check in addition to SNAP (SN Ia explorer) and CMB missions WMAP and Planck

Tegmak et al. 1998

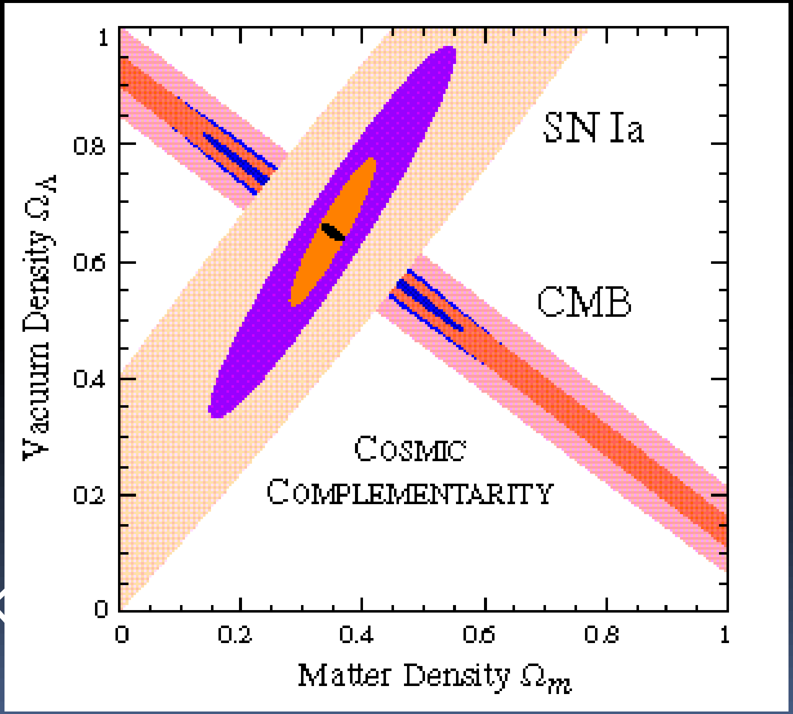

3σ

A glimpse of polarimetry

Stokes parameters – the "polarisation" language

The polarized state of a wave can be described in terms of 4 parameters, known as Stokes parameters:

I – the total energy flux or the 'total intensity'

Q, U – the linear polarization.

V – the circular polarization. $V \approx 0$ intrinsically for synchrotron radiation.

The complex polarization, P, is then given as

$$P = Q + iU = mIe^{2i\chi} = pe^{2i\chi}$$

where m is the fractional polarization, p is the polarized flux density and χ is the polarization position angle (= electric vector position angle, EVPA).

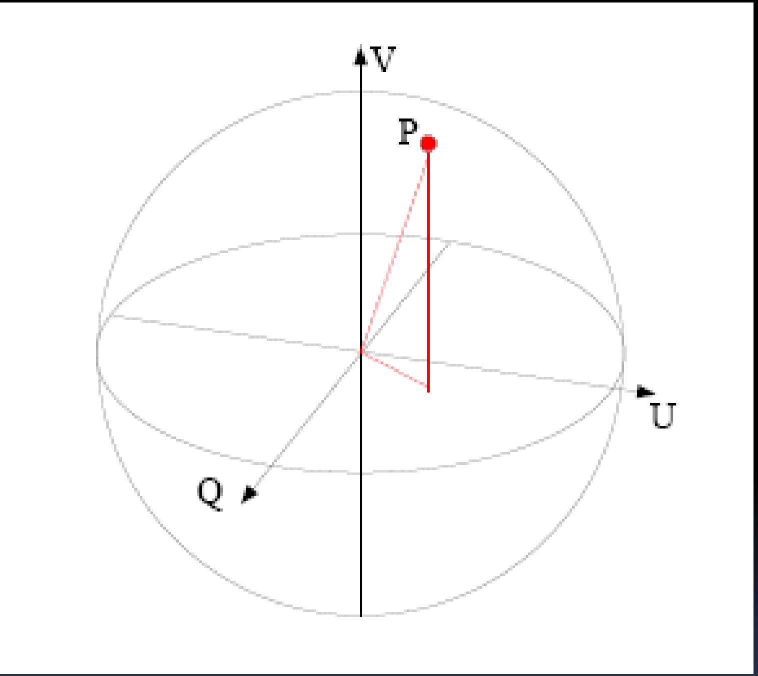

The Poincaré sphere provides a means for visualising the Stokes parameters. The point P represents a given polarization state and lies on the surface of the sphere whose radius is the total polarized power.

Stokes parameters and practical interferometry

Radio telescopes are equipped with either linearly or circularly polarized feeds. The correlations formed between the orthogonal modes are related to the Stokes as follows:

Circularly polarized feeds (most common in VLBI):

- Measure right circular polarization (RCP or R) and left circular polarization (LCP or L). The correlations that can be formed between antennas j and k are

$$R_j R_k^* = I + V$$
$$L_j L_k^* = I - V$$
$$R_j L_k^* = Q + iU$$
$$L_j R_k^* = Q - iU$$

Linearly polarized feeds (e.g. Westerbork, ATCA)

- Measure two perpendicular modes, p and q

$$p_j p_k^* = I + Q\cos 2\chi + U\sin 2\chi$$
$$q_j q_k^* = I - Q\cos 2\chi - U\sin 2\chi$$
$$p_j q_k^* = I - Q\sin 2\chi + U\cos 2\chi + iV$$
$$q_j p_k^* = I - Q\sin 2\chi + U\cos 2\chi - iV$$

Why celestial radio sources are polarised?

The radio emission from most bright radio sources arises from Synchrotron Radiation. Thus, it is linearly polarized.

The radiation from a single relativistic e^- gyrating around a magnetic field is elliptically polarized. For an ensemble of e^-'s with a smooth distribution of pitch angles the opposite senses of the elliptical polarization will cancel out resulting in linearly polarized radiation. If the e^-'s have a power law distribution the fractional polarization (m) in the presence of a uniform magnetic field is:

$$m = (\alpha + 1)/(\alpha + 5/3)$$

where α is the spectral index of the source. E.g. if $\alpha = 0.5$ (typical of synchroton emitting sources), $m = 0.7$.

Real radio sources generally have $m < 0.1 \Rightarrow$ tangled magnetic fields, cellular depolarization, Faraday depolarization, etc. Higher m can be seen as the result of 'repolarization'.

Depolarisation

- Experimental fact: celestial radio sources show low polarization compare with simple synchrotron models. Why?

Cellular depolarization:

Magnetic fields in the sources are not uniform but have small scale structures. Consider a source composed of many cells in each of which the magnetic field is randomly orientated. The polarization contribution from each cell adds *vectorially*. If there are N cells within the telescope beam, $m \rightarrow m/\sqrt{N}$.

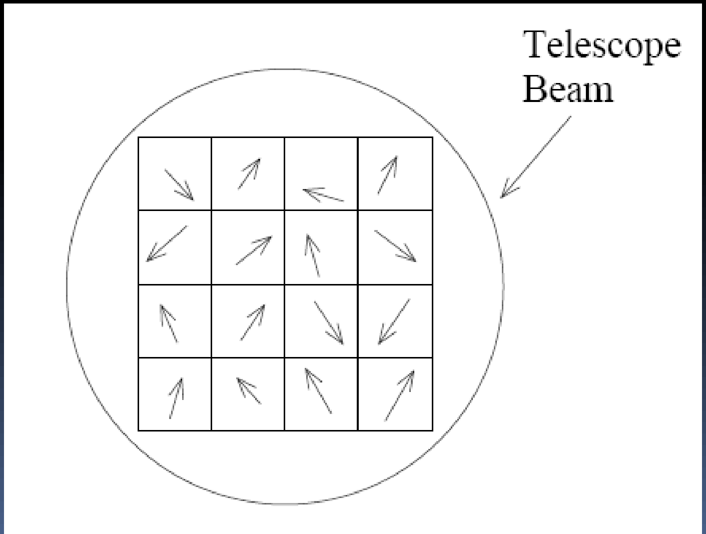

Arrows represent the dominant magnetic field direction in the cell.

Repolarisation

Repolarisation by field compression:
Compression of an initially random magnetic field (e.g. by a shock) modifies components of the field perpendicular to the direction of compression. A random field viewed along the axis of compression will still appear to be random. If a random field is compressed into a plane and is viewed in that plane, it will appear indistinguishable from an ordered field and will produce polarisation.

Laing 1980. MNRAS

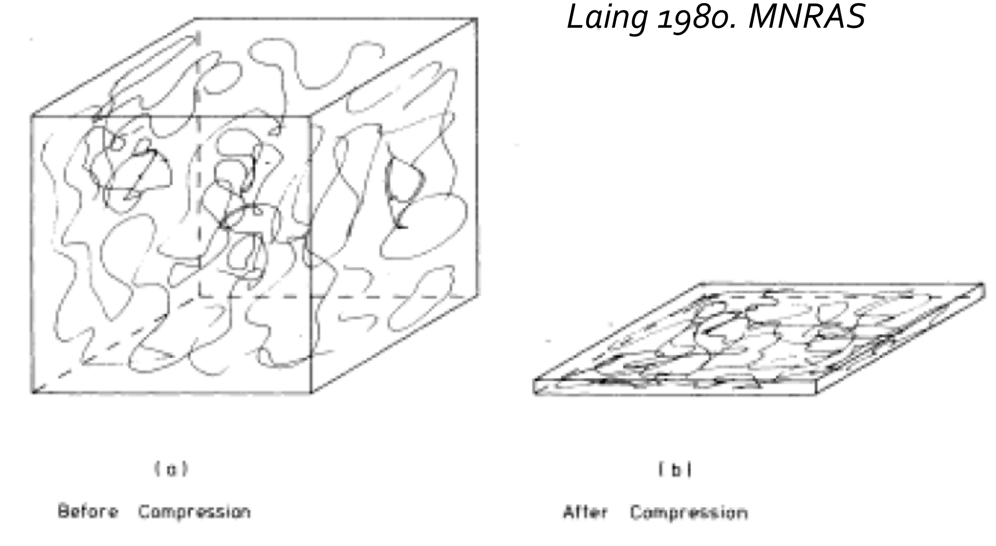

Repolarisation by field shear:
Shear layers result from the interaction between the surface of an expanding source and the surrounding medium. Essentially, a component of magnetic field gets 'stretched out' along the direction of motion in a boundary layer resulting in the development of a uniform component of magnetic field, with direction parallel to the direction of motion.

Faraday Rotation (qualitative description)

- Faraday rotation: rotation of the angle of polarization and occurs when electromagnetic radiation propagates through an ionised plasma containing cold (thermal) electrons and a magnetic field.

- For formal description: linearly poalrised emission to be de-composed into a superposiution of two cirtcularly polarised waves.

- Left- and right-circularly polarised waves propagate at different speeds through the plasma as they experience different refractive indices and this leads to a rotation of the angle of linear polarization. The rotation angle depends on the difference in velocity, Δv, as:

$$\theta = \frac{\pi}{\lambda} \int_0^D \frac{\Delta v}{c} \, ds$$

$$\theta = RM \, \lambda^2$$

$$RM = 8.1 \times 10^3 \int_0^D n_e B_{||} \, ds$$

where RM is the rotation measure (RM) in units of rad/m^2

Internal and External Faraday Rotation

- Faraday Rotation – effect of propagation
- Internal to the source medium – Internal FR
- External screen – External FR
- Vector nature of FR: vector sum within the beam
- Distinguishing between Internal and External FR is important for astrophysical interpretation:
  - Internal Faraday Rotation tends to induce depolarization and a departure from a simple λ^2 rotation as a result of the different path length through the Faraday screen which is traversed by radiation from the front and back of the source.
- For realistic geometries, internal Faraday rotation cannot produce a rotation greater than $\pi/2$ rads.

Radio astronomy of polarised radio emission

- Laing-Garrington effect
- Magnetic field alignments in quasar cores and lobes – helical fields?
- Faraday rotation as a probe of thermal gas content
- Kinematic constraints for parsec-scale jets
- Circular polarization has implications for jet composition – difficult to measure but may answer some important questions

- Polarisation gives information on the magnetic field orientation in the sources, the degree of ordering in the magnetic fields and the thermal gas content – much of this information cannot be obtained in any other way.

Laing-Garrington Effect

The cause of the one-sidedness in the jets of otherwise symmetrical extragalactic radio sources – higher degree of depolarisation for the receding jet (greater optical depth through the intrinsic depolarising medium of the source):

Circumstantial confirmation for the Doppler boosting explanation of one-sidedness of extragalactic jets

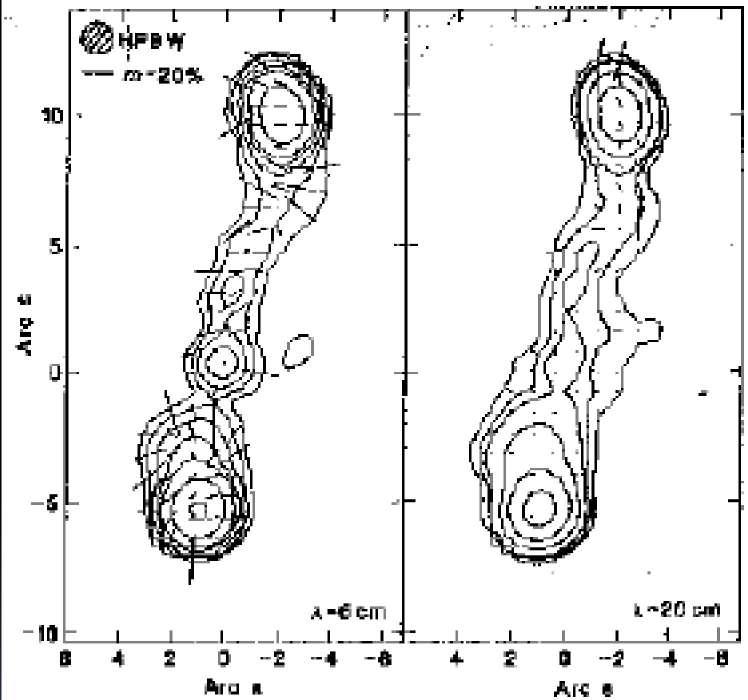

Fig. 1 Maps of 4C16.49 (1732+16) at 6 cm (left) and 20 cm (right). Contours give total intensity; the bars give the direction of the E-field of the polarized radiation, with their lengths proportional to the fractional polarization. The half power beamwidth (HPBW) is 1.3 arc s and coordinates are given relative to the position of the optical quasar. The jet points to the northern component; marked depolarization occurs on the south side, but not on the north side of the source.

Garrington et al. 1988, Nature

Importance of high angular resolution

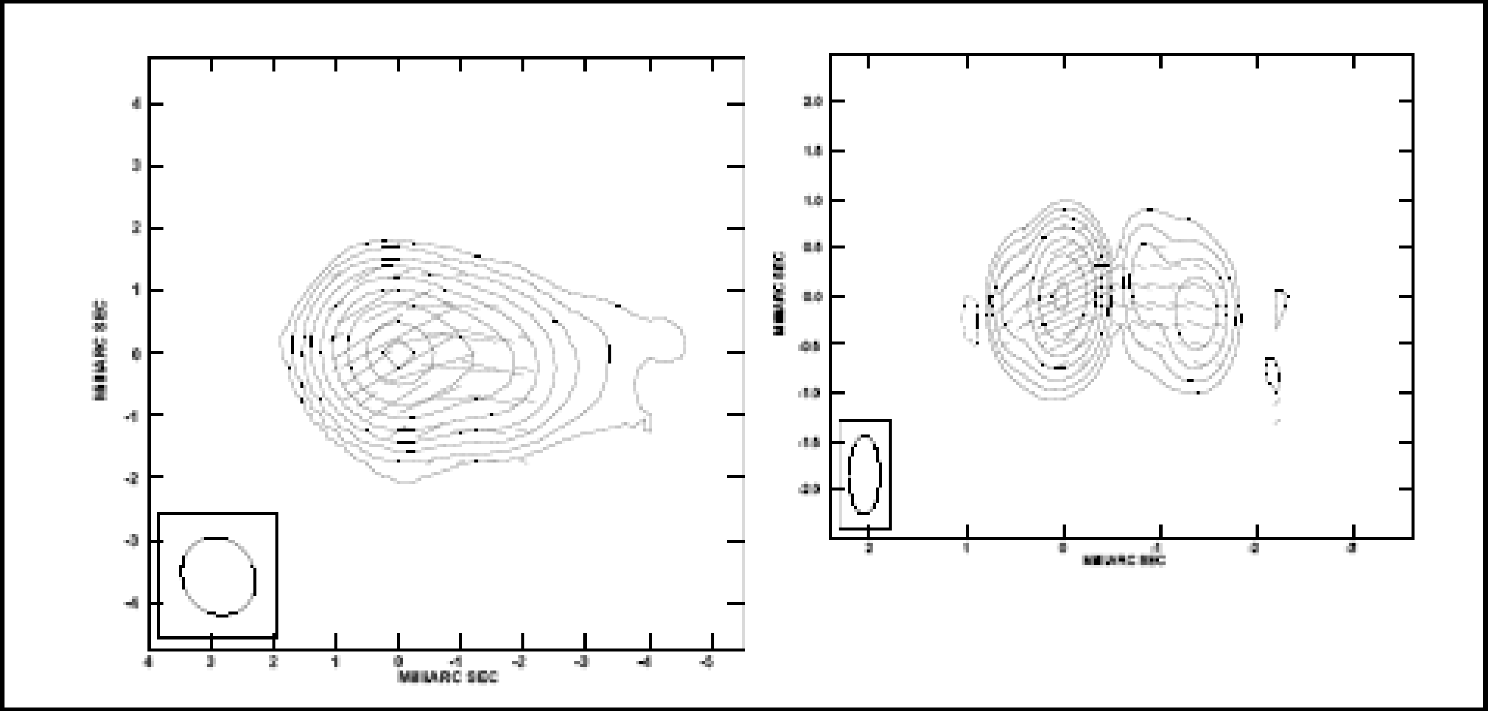

The map on the left is 1803+784 at 5 GHz observed with the VLBA. The contours are of total intensity and the overlaid sticks indicate the polarized ntensity and EVPA. The map on the right uses the same data, but with the addition of (v. long) baselines to the orbiting VLBI antenna HALCA. The improved resolution given by the space baselines allow one to see that the electric vectors very neatly follow the bend in the jet with no evidence for misalignments (Gabuzda 1999, NewAR, 43, 695).

Polarisation VLBI (aka VLBP)

- Considered to be a 'black-belt' level of the VLBI art
  - Polarised emission accounts for single-digit percents of the total flux density - the problem of sensitivity!
  - The amount of data is 4 times larger than that of "total intensity" VLBI (LL, RR, LR and RL visibilities)
  - Data processing involves additional polarisation-specific calibrations, such as
    - *Instrumental polarisation effects*
    - *Polarisation position angle calibration*

- But VLBP is perfectly doable – even by students!
- Further reading: Gabuzda in "Radio Astronomy from Karl Jansky to Microjansky", p. 109

Active Galactic Nuclei and we: a few concluding facts

- Strange coincidences – cosmic conspiracy?
  - 10^{12} K is about the maximum measurable brightness temperature with the baseline ~10,000 km. We happen to live on the "interferometrically" correct planet!
  - The most compact structures in AGN begin to appear at baselines ~200 Mλ (1 mas), just a bit longer than available on the Earth at 5 GHz, the most popular VLBI frequency of the recent past. Again, we live on a very special planet!
- Both the items above have become known to us essentially owing to baselines longer than the Earth diameter (VSOP).
- Radio structures < 1 mas are likely to be the last bastion on the way to complete resolution of the cores – definitive diagnostics of the "SMBH – accretion disc – jet" system.
- Baselines 10,000 – 100,000 km (Space VLBI) and sub-mJy sensitivity are crucial!

Some questions (for curious radio astronomers)

- What triggers AGN activity?
- Why are some galaxies active and others not (fortunately, our Milky Way is NOT an active galaxy)?
- How frequent are AGN outburst, and how long do they take?
- What are the jets made of?
- How is the massive black hole formed?
- What is its relation between the nucleus and the host galaxy?
- How energy is transported from the nucleus to the jet?

Next generation of radio astronomy facilities might help to find the answers!

Huygens VLBI heritage: 20 photons/dish/s

- Ad hoc use of the Huygens “uplink” carrier signal at 2040 MHz
- Utilised 17 Earth-based radio telescopes
- Non-optimal parameters of the experiment (not planned originally)
- Achieved 1 km accuracy of Probe’s descent trajectory determination
- Assisted in achieving one of main science goals of the mission – vertical wind profile

3D Huygens descent trajectory

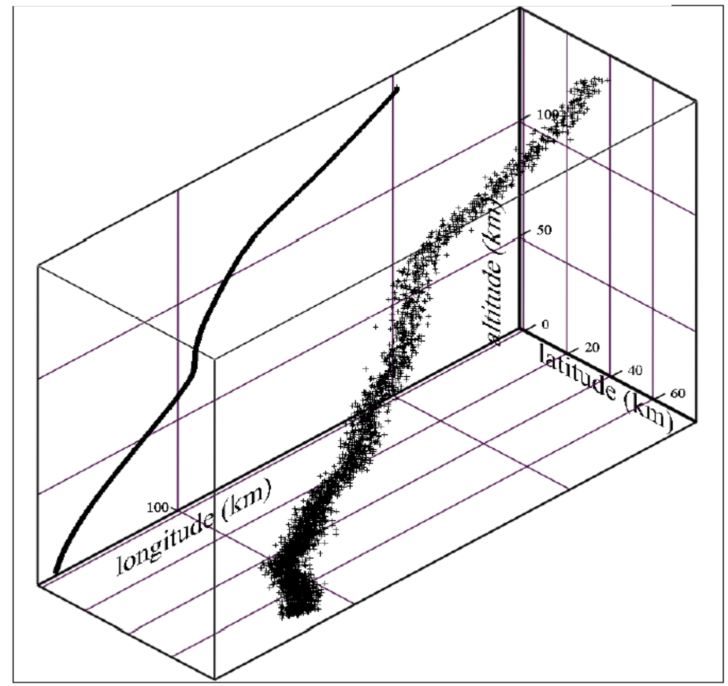

Titan atmosphere turbulence signature

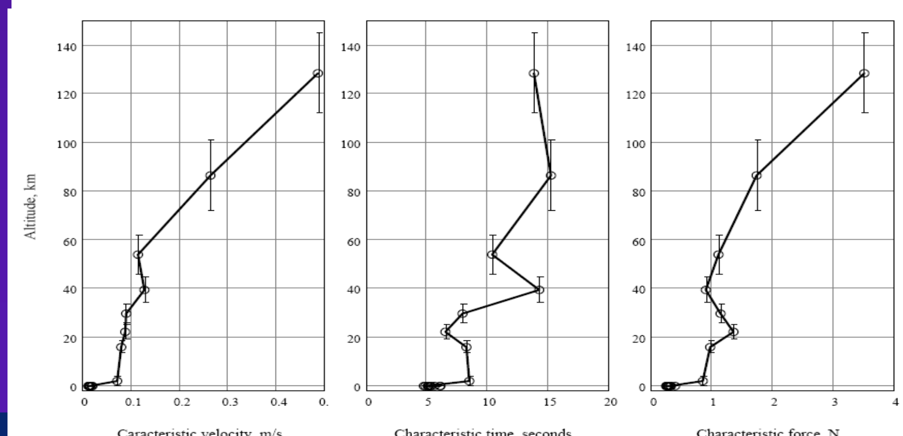

Expect unexpected spin-offs…

Water maser detection near Enceladus – as a Huygens VLBI tracking spin-off

(spectral line single dish experiment in VLBI continuum mode…)

~350 "in gap" hrs at Medicina and Metsähovi; in collaboration with INAF, HUT, U Kentucky

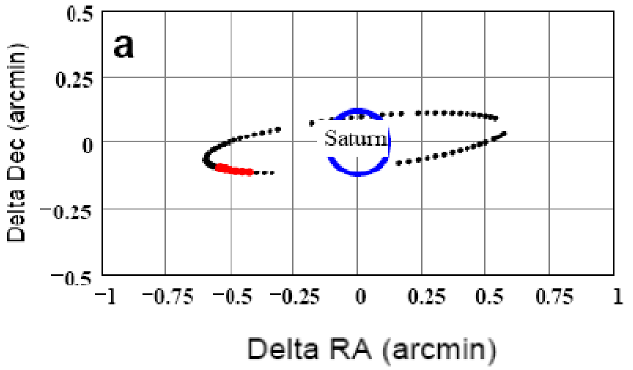

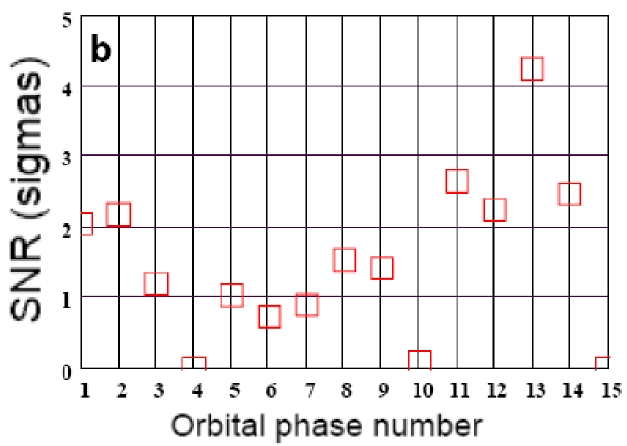

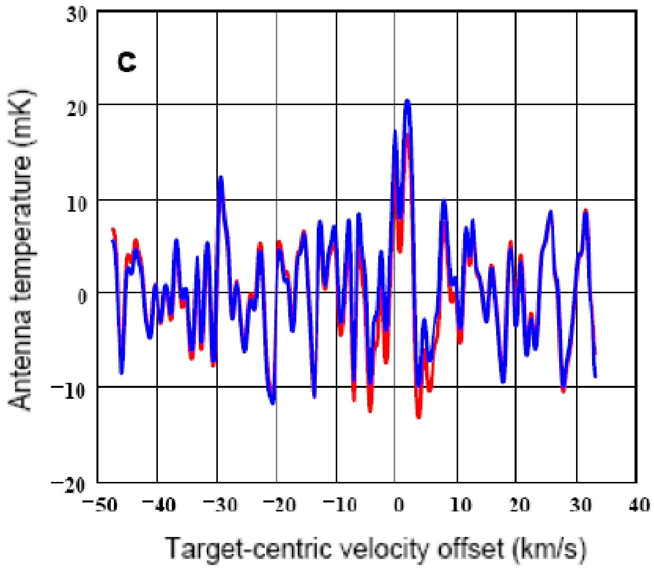

- ***Puzzling physics***
- ***Ongoing study***

Pogrebenko et al. 2009, IAU Symp 263 (Rio), in press

Water masers near Hyperion and Titan

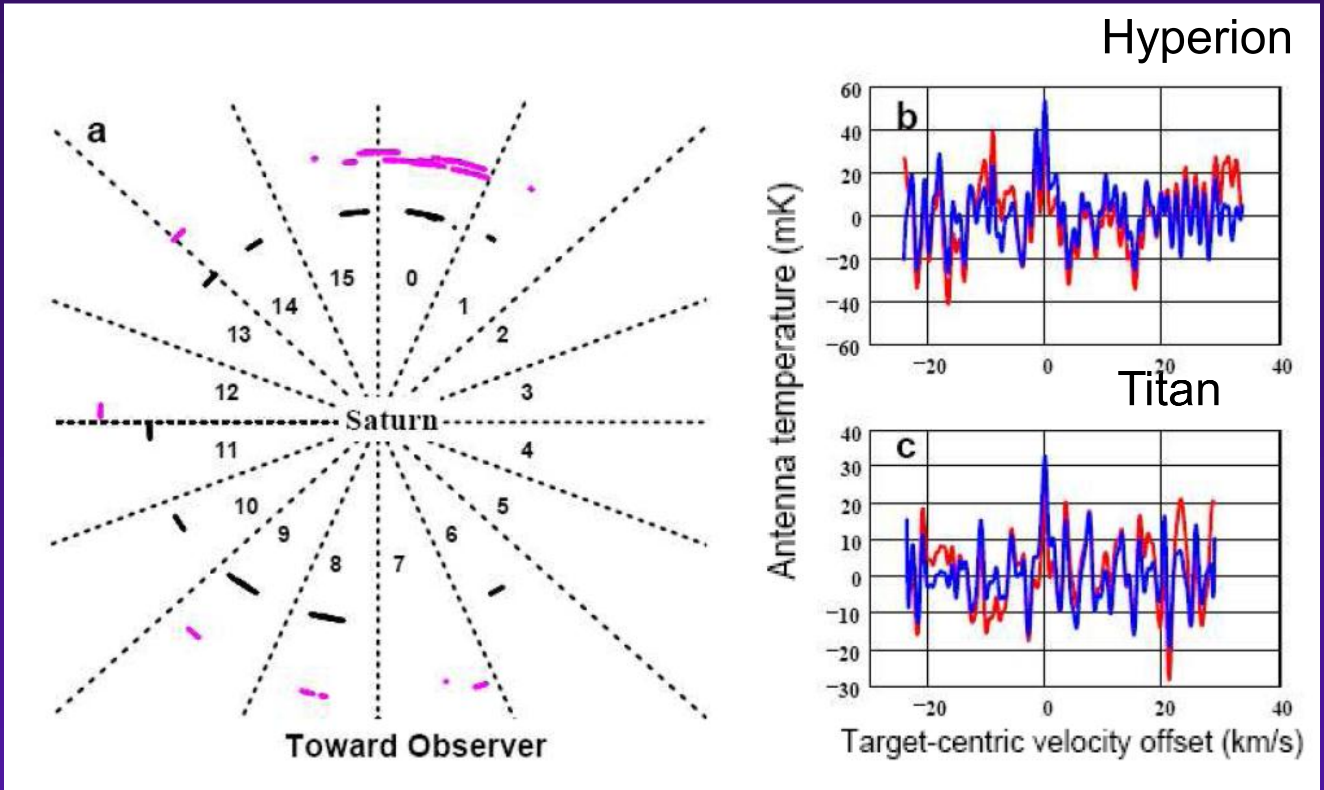

Sponge-like shape of Hyperion: result of selective sublimation of ice, enhanced by interaction with Solar wind when the satellite is outside the Kronian magnetosphere?

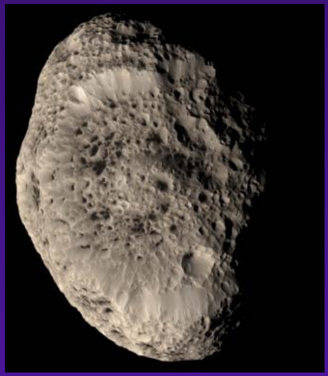

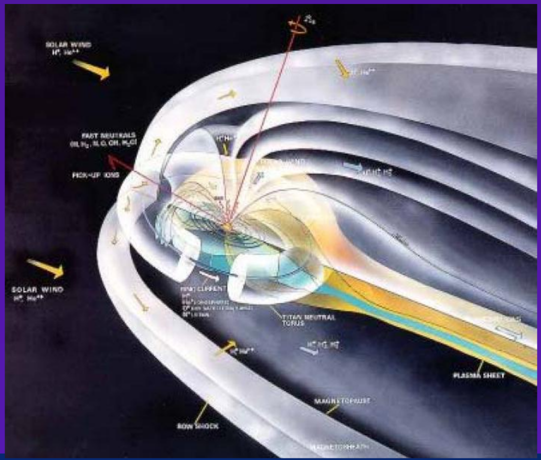

Kronian magnetosphere:
a suitable masing machine?

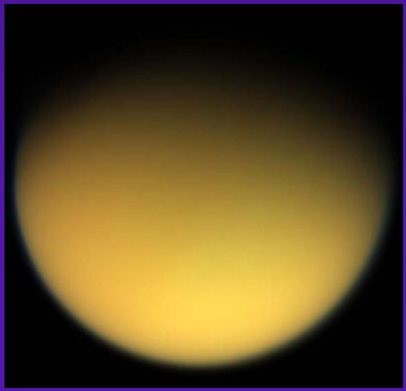

Titan: collisional pumping for trapped water molecules?